Research Square

Preprints are preliminary reports that have not undergone peer review.
They should not be considered conclusive, used to inform clinical practice,
or referenced by the media as validated information.

Ulnar Shortening Osteotomy for Ulnar Impaction Syndrome Adjust the Wrist Joint

Mitsutoshi Ota
Hokkaido University
Kyosuke Numaguchi
Hokkaido University
Daisuke Momma
d-momma@med.hokudai.ac.jp

Hokkaido University Hospital
Eiji Kondo
Hokkaido University Hospital
Norimasa Iwasaki
Hokkaido University

Article

Keywords:

Posted Date: April 1st, 2026

DOI: https://doi.org/10.21203/rs.3.rs-8904966/v1

License: This work is licensed under a Creative Commons Attribution 4.0 International License. Read Full License

Additional Declarations: No competing interests reported.

Abstract

Ulnar shortening osteotomy is widely performed as a surgical treatment for ulnar impaction syndrome, however, the in vivo effects of ulnar shortening osteotomy for ulnar impaction syndrome on the wrist joint remain unclear. We hypothesized that the in vivo effects of the wrist joint could be evaluated using a custom-designed analytical program. The aim of the study was to compare the articular contact area of the wrist joint before and after ulnar shortening osteotomy for ulnar impaction syndrome. 16 wrists of 13 patients underwent ulnar shortening osteotomy for ulnar impaction syndrome. Computed tomography (CT) images of the wrist joint were reconstructed using a 3D reconstruction software package. Radioscaphoid, radiolunate, and distal radioulnar joint contact areas and translation of the contact area, scaphoid, lunate, and triquetrum centroid from preoperative to postoperative were calculated using customized software. All patients reported a marked reduction in wrist pain at the 12-month follow-up. The distal radioulnar joint contact area was significantly increased following ulnar shortening, and the centroid of the distal radioulnar joint was translated to volar and proximal postoperatively. CT-based analysis revealed that the contact area changed following ulnar shortening osteotomy. Ulnar shortening osteotomy altered the contact area and carpal bone translation.

Study Type: Diagnostic Case-control Study; Level III

Introduction

Ulnar impaction syndrome (UIS) is a degenerative condition of the ulnar side of the wrist caused by excessive load transmission between the distal ulna, the triangular fibrocartilage complex (TFCC), and the ulnocarpal joint[1]. Repetitive mechanical stress on these structures may lead to progressive degeneration of the TFCC and ulnocarpal cartilage, resulting in ulnar-sided wrist pain, reduced motion, and functional impairment. Positive ulnar variance is considered one of the major anatomical factors contributing to increased load across the ulnocarpal articulation.

Ulnar shortening osteotomy (USO) is widely performed to treat UIS when nonoperative management fails. By shortening the ulna, this procedure reduces load transmission through the TFCC and ulnocarpal joint and is associated with favorable clinical outcomes, including pain relief and improved wrist function[2,3]. Although the clinical effectiveness of USO has been well documented, the biomechanical mechanisms underlying symptom improvement remain incompletely understood[4,5].

Previous biomechanical investigations have primarily relied on cadaveric experiments or theoretical models to estimate load transmission within the wrist joint[6]. While these studies have provided important insights into wrist mechanics, experimental models cannot fully reproduce the physiological joint conditions present in living subjects[7,8]. Consequently, direct in vivo evaluation of joint surface interaction and load distribution following USO remains limited.

Quantitative assessment of articular contact patterns provides valuable information regarding joint biomechanics because contact area and its spatial distribution reflect how load is transmitted across the articular surfaces[9]. Recent advances in computed tomography (CT)–based three-dimensional (3D) bone modeling have enabled detailed in vivo analysis of joint morphology and contact characteristics. These techniques allow reconstruction of patient-specific bone geometry and facilitate quantitative evaluation of articular surface relationships within the wrist.

Using CT-based 3D modeling, it is possible to estimate joint contact areas and analyze spatial changes in articular contact following surgical intervention. Such analyses may provide new insights into how surgical procedures modify joint mechanics and redistribute load across the wrist.

The purpose of this study was to investigate changes in wrist joint contact areas and carpal bone position before and after USO in patients with UIS using CT-based three-dimensional bone models. We hypothesized that USO would alter the distribution of articular contact within the wrist joint and modify the spatial relationship of the carpal bones.

Materials and Methods

Ethics statement

This study was conducted in accordance with the Declaration of Helsinki and all relevant guidelines and regulations. The study protocol was approved by the Institutional Review Board of Hokkaido University Hospital (approval ID: 024–0312). Written informed consent was obtained from all participants prior to inclusion in the study.

Patients

All patients underwent USO between 2011 and 2017 for the treatment of UIS. Computed tomography, plain X-rays, and clinical assessment data were collected pre- and postoperatively. The Modified Mayo Wrist Scoring system was used for pre- and postoperative assessment of pain and wrist range of motion (ROM).

Surgical technique

All surgical procedures were performed under general anesthesia by three specialists in hand surgery (N.I., Y.M., D.K.). Details of the surgical procedure have been described previously[5]. After the arthroscopic procedures were complete, USO was performed by making two parallel transverse cuts to remove a segment of the bone, the length of which equaled the amount of positive ulnar variance measured on preoperative radiographs, taking into consideration the thickness of the saw blade. Fixation at the osteotomy site was accomplished using a six-hole small dynamic compression plate (LC-DCP; Synthes, West Chester, PA, USA). A volar short-arm splint was applied for 2 weeks after surgery, followed by active and passive motion according to the severity of pain. Full activity was resumed after bone healing, which took approximately 3 months.

3D bone model creation

CT images were obtained with a 320-slice multidetector scanner with a wide field-of-view (FOV) (Aquilion One; Canon Medical Systems, Tochigi, Japan; slice thickness, 0.5 mm; slice interval, 0.5 mm; matrix 512 · 512; FOV φ500 mm). Axial CT images of the wrist were obtained before surgery and at 12 months postoperatively. Due to the use of a titanium fixation plate in all patients, there was no CT image degradation due to metal artifact. CT images of each wrist joint were imported in DICOM format and segmented using segmentation software (Mimics 21R; Materialise, Leuven, Belgium). Three-dimensional images of the radius, scaphoid, lunate, and ulna were reconstructed, and the resulting 3D models were then exported as pointcloud and polygon models using the same software. The 3D radius, scaphoid, lunate, and ulna bone models were then analyzed with custom-written software created using Microsoft Visual C + + in the Microsoft Foundation Class programming environment (Microsoft, Redmond, WA, USA) for further analysis[10–12].

Definition of joint contact area and anatomical coordinate system

The surface-to-surface least-distance distributions between the radius and scaphoid models, between the radius and lunate models, and between the radius and ulna models were calculated by a point-to-surface distance calculation algorithm using custom-written software[13]. Articular contact areas were defined as areas where the least distances were under a certain threshold level. The distance thresholds were determined with reference to previous studies of distances within the wrist joint space[11,14]. The threshold was 2.0 mm for each of the radioscaphoid, radiolunate, and distal radioulnar joints. The radioscaphoid, radiolunate, and distal radioulnar joint contact areas were calculated from the 3D bone models using custom-written software. The center of the contact area was also calculated, and preoperative to postoperative translation was calculated using custom-written software. To evaluate translation of the center of the contact area, a validated 3D–3D registration method was used and a preoperative-to-postoperative transformation matrix was obtained[15,16]. We used the standard anatomical coordinate system for the wrist of the International Society of Biomechanics (Fig. 1)[17].

Statistical Analysis

We compared the Modified Mayo Wrist Scores, ulnar variance, and the contact area between preoperative and postoperative measurements using a paired t test. P values < .05 were considered significant. Data are presented as mean ± SD and the corresponding 95% confidence intervals. All statistical analyses were conducted using statistical software JMP Pro 16.0 (SAS Institute, Cary, NC, USA).

Results

Participant demographics

Sixteen wrists of 13 patients underwent USO for UIS (Table 1). All patients reported a marked reduction in wrist pain at the 12-month follow-up. Radiographic evaluation showed that none of the patients had postoperative osteoarthritic changes, such as bony spur formation, within the follow-up period. The mean preoperative ulnar variance on posteroanterior X-rays was + 3.2 mm[18]. The postoperative value was + 1.1 mm ($p < .01$)[18]. The average postoperative range of extension and flexion of the wrist increased from 139.7° to 159.1° ($p = 0.02$). All patients except three were graded as excellent or good according to the Modified Mayo Wrist Scoring system. The mean Modified Mayo Wrist Score was significantly improved from 61.9 preoperatively to 88.4 at final follow-up ($p < .01$).

Table 1
Characteristics of the Study Participants

Case			Affected	Ulnar Variance		Range of motion		Modified Mayo Wrist Score	
	Sex	Age	Hand	Pre-operation	Post-operation	Pre-operation	Post-operation	Pre-operation	Post-operation
1	Male	31	L	3.1	0.5	180	180	80	90
2	Male	37	L	3.5	1.0	160	180	65	95
3	Female	51	R	2.7	0.7	30	140	5	65
4	Female	55	L	3.4	1.5	165	180	40	75
	Female	55	R	4.6	1.7	150	160	30	75
5	Female	37	R	1.7	-0.3	160	180	70	95
6	Female	28	L	4.5	0.3	95	145	70	100
7	Male	46	R	2.3	0.3	160	170	80	90
8	Female	63	L	5.0	4.0	160	160	65	90
	Female	63	R	5.1	4.0	140	150	75	85
9	Female	56	L	2.4	0.3	160	160	70	100
	Female	56	R	1.6	-0.4	160	160	70	100
10	Female	51	R	1.1	-0.9	130	180	65	100
11	Male	56	R	1.8	0.2	140	170	75	85
12	Male	45	R	3.7	1.0	115	110	70	80
13	Male	59	R	5.2	3.0	130	120	60	90
Mean		49.3 ± 10.9		3.2 ± 1.4	1.1 ± 1.5	140.0 ± 36.2	159.0 ± 21.6	61.9 ± 20.2	88.4 ± 10.4
p value pre- vs post-operation					< .01		0.021		< .01

Joint contact area

The contact area of the radioscaphoid joint changed from 211.7 ± 64.5 mm^2 to 217.0 ± 54.2 mm^2 postoperatively (Fig. 2, Table 2). The contact area of the radiolunate joint changed from 186.4 ± 50.9 mm^2 to 181.3 ± 54.7 mm^2 postoperatively. There were no statistically significant differences. By contrast, the contact area of the distal radioulnar joint showed a significant increase from 90.4 ± 28.4 mm^2 to 105.8 ± 32.9 mm^2 postoperatively ($p = 0.046$).

Table 2
Joint contact area

Case	Affected	Radioscaphoid joint		Radiolunate joint		Distal radioulnar joint	
	Hand	Pre-operation	Post-operation	Pre-operation	Post-operation	Pre-operation	Post-operation
1	L	140.1	119.5	152.3	143.5	54.1	101.3
2	L	180.8	186.9	138.9	127.0	77.1	80.9
3	R	211.8	223.6	140.6	157.0	59.6	65.1
4	L	159.0	168.4	139.4	132.0	65.3	57.8
	R	118.2	170.0	152.5	96.0	67.7	75.9
5	R	246.5	252.7	218.3	167.5	123.1	64.9
6	L	159.8	177.2	130.6	134.9	61.8	90.5
7	R	210.0	200.3	230.6	216.8	111.0	122.2
8	L	192.6	260.4	239.6	271.7	118.1	143.7
	R	224.9	230.3	273.1	260.3	115.8	144.6
9	L	206.5	198.8	199.1	142.7	56.7	116.6
	R	220.5	200.8	207.9	170.0	107.2	126.3
10	R	181.6	192.6	203.8	218.3	96.5	144.5
11	R	303.9	328.0	253.7	259.3	98.4	164.3
12	R	383.6	313.2	203.8	235.5	147.4	99.9
13	R	247.1	249.0	98.1	168.9	87.3	93.7
Mean ± SD		211.7 ± 64.5	217.0 ± 54.2	186.4 ± 50.9	181.3 ± 54.7	90.4 ± 28.4	105.8 ± 32.9
p value pre- vs post-operation			0.285		0.250		0.046

Centroids of joint contact areas

The postoperative translations of the radioscaphoid, radiolunate, and distal radioulnar joint centroids were decomposed into radial, volar, and distal directions. Radioscaphoid joint translation: The ulnar translation distance was 0.13 ± 0.6 mm, the volar translation distance was 0.20 ± 0.7 mm, and the proximal translation distance was 0.09 ± 0.3 mm (Fig. 3). Radiolunate joint translation: The ulnar translation distance was 0.13 ± 0.6 mm, the volar translation distance was 0.28 ± 0.6 mm, and the proximal translation distance was 0.09 ± 0.3 mm. Distal radioulnar joint translation: The ulnar translation distance was 0.09 ± 0.3 mm, the volar translation distance was 0.66 ± 1.0 mm, and the proximal translation distance was 0.61 ± 1.1 mm.

Centroids of carpal bones

The postoperative translations of the scaphoid, lunate, and triquetrum centroids were decomposed into radial, volar, and distal directions. Scaphoid translation: The ulnar translation distance was 0.47 ± 1.3 mm, the volar translation distance was 0.44 ± 0.9 mm, and the proximal translation distance was 0.09 ± 0.3 mm (Fig. 4). Lunate translation: The

ulnar translation distance was 0.33 ± 1.1 mm, the volar translation distance was 0.09 ± 0.4 mm, and the proximal translation distance was − 0.08 ± 0.4 mm. Triquetrum translation: The ulnar translation distance was 0.37 ± 1.2 mm, the volar translation distance was 0.31 ± 0.8 mm, and the proximal translation distance was 0.40 ± 1.4 mm.

Discussion

The present study used patient-specific CT-based three-dimensional bone models to investigate biomechanical changes in the wrist following USO for UIS. By quantifying articular contact areas and spatial displacement of carpal bones before and after surgery, this analysis provides in vivo information on how USO modifies joint mechanics within the wrist.

UIS is generally attributed to excessive load transmission between the distal ulna, the triangular fibrocartilage complex (TFCC), and the ulnocarpal articulation. Surgical shortening of the ulna has been widely used to reduce this mechanical overload and to relieve ulnar-sided wrist pain. Although favorable clinical outcomes after USO have been consistently reported, the mechanisms by which the procedure alters load transmission within the wrist have not been fully clarified[7,19]. In particular, direct in vivo evaluation of joint surface interaction after USO has been limited because measuring articular contact characteristics under physiological conditions is technically challenging.

Three-dimensional CT–based modeling techniques have recently made it possible to estimate joint surface relationships and contact patterns in living subjects. These approaches allow detailed assessment of joint congruity and spatial alignment of bones without relying on cadaveric simulations. By applying this method to wrists treated with USO, the present study was able to quantify changes in both joint contact areas and the position of carpal bones relative to the distal radius and ulna.

One of the notable findings of this investigation was the shift in the spatial distribution of articular contact within the wrist. After USO, the centroid of the joint contact area demonstrated a tendency to move toward the ulnar and volar directions. In parallel with these changes in contact location, the centroids of the carpal bones also exhibited a postoperative translation toward the volar side. These observations suggest that shortening of the ulna modifies the alignment of the wrist joint and alters how the articular surfaces interact during physiological loading[20–22].

Among the evaluated joints, the distal radioulnar joint showed the most prominent change in contact characteristics. Following surgery, the contact area at the distal radioulnar joint increased and its centroid shifted in the volar and proximal directions. This pattern may reflect improved congruity between the distal radius and ulna after shortening of the ulna, resulting in redistribution of contact across a broader articular surface[21]. A larger contact area may contribute to a reduction in focal stress within the TFCC and adjacent structures.

From a biomechanical perspective, these findings indicate that USO modifies wrist load transmission by altering both the spatial distribution of joint contact and the position of the carpal bones[22]. Our findings indicate that USO alters the spatial distribution of articular contact within the wrist. Following surgery, the location of the contact area shifted toward the ulnar and volar directions, accompanied by a volar translation of the carpal bones. In addition, the distal radioulnar joint contact area shifted toward the volar and proximal directions after surgery. Taken together, these changes suggest that shortening of the ulna modifies the interaction between the distal radius, ulna, and carpal bones.

Clinically, all patients in the present series were able to return to their previous activities without functional limitations of the wrist. The observed biomechanical changes may therefore provide a mechanical explanation for the favorable clinical outcomes associated with USO[23,24]. By modifying articular contact distribution and carpal alignment, the

procedure appears to alter the mechanical environment of the ulnar side of the wrist. These findings support the concept that USO reduces mechanical loading on the TFCC by changing joint contact patterns and carpal bone position[25,26]. Taken together, these findings suggest that shortening of the ulna modifies load transmission across the ulnar side of the wrist, which may contribute to mechanical decompression of the TFCC.

Several limitations of this study should be considered. First, the analysis was based on CT-derived bone models and therefore did not directly evaluate cartilage thickness or soft tissue structures, including the TFCC. Second, the number of included patients was relatively small, which may limit the generalizability of the findings. Third, joint contact areas were estimated using a distance threshold between articular surfaces rather than direct measurement of contact pressure. Despite these limitations, the use of in vivo three-dimensional modeling allowed a detailed assessment of wrist joint mechanics after USO. Future studies with larger cohorts and additional biomechanical parameters may further clarify how surgical correction influences load distribution within the wrist.

In summary, CT-based three-dimensional analysis demonstrated that ulnar shortening osteotomy alters the spatial characteristics of joint contact within the wrist and induces volar translation of the carpal bones. These biomechanical changes suggest that the procedure modifies load transmission across the ulnar side of the wrist and may contribute to mechanical decompression of the TFCC.

Declarations

Funding Declaration

There was no Funding.

Author Contribution

M.O. and D.M. participated in the design of the study and carried out the experiments and statistical analysis. D.M. drafted the manuscript. K.N. and N.I. assisted in carrying out the experiments and with the manuscript preparation. E.K., and N.I. conceived of the study and provided assistance.

References

1. Darrow, J. C., Jr. et al. Distal ulnar recession for disorders of the distal radioulnar joint. J Hand Surg Am 10, 482-491, doi:10.1016/s0363-5023(85)80069-1 (1985).
2. Minami, A. & Kato, H. Ulnar shortening for triangular fibrocartilage complex tears associated with ulnar positive variance. J Hand Surg Am 23, 904-908, doi:10.1016/S0363-5023(98)80171-8 (1998).
3. Deshmukh, S. C., Shanahan, D. & Coulthard, D. Distal radioulnar joint incongruity after shortening of the ulna. J Hand Surg Br 25, 434-438, doi:10.1054/jhsb.2000.0456 (2000).
4. Nishiwaki, M., Nakamura, T., Nakao, Y., Nagura, T. & Toyama, Y. Ulnar shortening effect on distal radioulnar joint stability: a biomechanical study. J Hand Surg Am 30, 719-726, doi:10.1016/j.jhsa.2005.04.015 (2005).
5. Hasegawa, Y., Matsui, Y. & Iwasaki, N. Computed tomography osteoabsorptiometry changes following ulnar shortening osteotomy: observations in nine patients. J Hand Surg Eur Vol 45, 527-529, doi:10.1177/1753193420908795 (2020).
6. Abe, S. et al. Three-Dimensional In Vivo Analysis of Malunited Distal Radius Fractures With Restricted Forearm Rotation. J Orthop Res 37, 1881-1891, doi:10.1002/jor.24332 (2019).

7. Palmer, A. K. & Werner, F. W. Biomechanics of the distal radioulnar joint. Clin Orthop Relat Res, 26-35 (1984).
8. Baek, G. H. et al. Ulnar shortening osteotomy in idiopathic ulnar impaction syndrome. J Bone Joint Surg Am 87, 2649-2654, doi:10.2106/JBJS.D.02983 (2005).
9. Bey, M. J., Kline, S. K., Zauel, R., Kolowich, P. A. & Lock, T. R. In Vivo Measurement of Glenohumeral Joint Contact Patterns. EURASIP J Adv Signal Process 2010, doi:10.1155/2010/162136 (2010).
10. Numaguchi, K. et al. Changes in elbow joint contact area in symptomatic valgus instability of the elbow in baseball players. Sci Rep 11, 19782, doi:10.1038/s41598-021-99193-0 (2021).
11. Shiota, J. et al. Changes in wrist joint contact area following radial shortening osteotomy for Kienbock's disease. Sci Rep 12, 4001, doi:10.1038/s41598-022-08027-0 (2022).
12. Irie, T. et al. Three-dimensional hip joint congruity evaluation of the borderline dysplasia: Zonal-acetabular radius of curvature. J Orthop Res 38, 2197-2205, doi:10.1002/jor.24631 (2020).
13. Irie, T. et al. Three-dimensional curvature mismatch of the acetabular radius to the femoral head radius is increased in borderline dysplastic hips. PLoS One 15, e0231001, doi:10.1371/journal.pone.0231001 (2020).
14. Ranota, P., Zhang, Y., Lalone, E. A. & Suh, N. Four-Dimensional Computed Tomography to measure distal radial-ulnar and radio-carpal joint congruency following distal radius fractures. J Orthop 25, 31-39, doi:10.1016/j.jor.2021.03.008 (2021).
15. Forsythe, B. et al. Dynamic 3-Dimensional Mapping of Isometric Anterior Cruciate Ligament Attachment Sites on the Tibia and Femur: Is Anatomic Also Isometric? Arthroscopy 34, 2466-2475, doi:10.1016/j.arthro.2018.03.033 (2018).
16. Forsythe, B. et al. Dynamic Three-Dimensional Computed Tomography Mapping of Isometric Posterior Cruciate Ligament Attachment Sites on the Tibia and Femur: Single- Versus Double-Bundle Analysis. Arthroscopy 36, 2875-2884, doi:10.1016/j.arthro.2020.06.006 (2020).
17. Wu, G. et al. ISB recommendation on definitions of joint coordinate systems of various joints for the reporting of human joint motion--Part II: shoulder, elbow, wrist and hand. J Biomech 38, 981-992, doi:10.1016/j.jbiomech.2004.05.042 (2005).
18. Gartland, J. J., Jr. & Werley, C. W. Evaluation of healed Colles' fractures. J Bone Joint Surg Am 33-a, 895-907 (1951).
19. Linscheid, R. L. Biomechanics of the distal radioulnar joint. Clin Orthop Relat Res, 46-55 (1992).
20. Tencer, A. F. et al. Pressure distribution in the wrist joint. J Orthop Res 6, 509-517, doi:10.1002/jor.1100060406 (1988).
21. Iwasaki, N., Genda, E., Minami, A., Kaneda, K. & Chao, E. Y. Force transmission through the wrist joint in Kienbock's disease: a two-dimensional theoretical study. J Hand Surg Am 23, 415-424, doi:10.1016/S0363-5023(05)80459-9 (1998).
22. Padmore, C. E., Chan, A. H. W., Langohr, G. D. G., Johnson, J. A. & Suh, N. The Effect of Forearm Position on Wrist Joint Biomechanics. J Hand Surg Am 46, 425 e421-425 e410, doi:10.1016/j.jhsa.2020.10.017 (2021).
23. Chun, S. & Palmer, A. K. The ulnar impaction syndrome: follow-up of ulnar shortening osteotomy. J Hand Surg Am 18, 46-53, doi:10.1016/0363-5023(93)90243-V (1993).
24. Teunissen, J. S. et al. Outcomes of ulna shortening osteotomy: a cohort analysis of 106 patients. J Orthop Traumatol 23, 1, doi:10.1186/s10195-021-00621-8 (2022).
25. Viegas, S. F., Wagner, K., Patterson, R. & Peterson, P. Medial (hamate) facet of the lunate. J Hand Surg Am 15, 564-571, doi:10.1016/s0363-5023(09)90016-8 (1990).

26. Barbaric, K., Rujevcan, G., Labas, M., Delimar, D. & Bicanic, G. Ulnar Shortening Osteotomy After Distal Radius Fracture Malunion: Review of Literature. Open Orthop J 9, 98-106, doi:10.2174/1874325001509010098 (2015).

Figures



Figure 1

Anatomical coordinate system of the wrist. Translations along the X-, Y-, and Z-axes indicate the radial (+)/ulnar (−), dorsal (+)/volar (−), and distal (+)/proximal (−) directions, respectively.

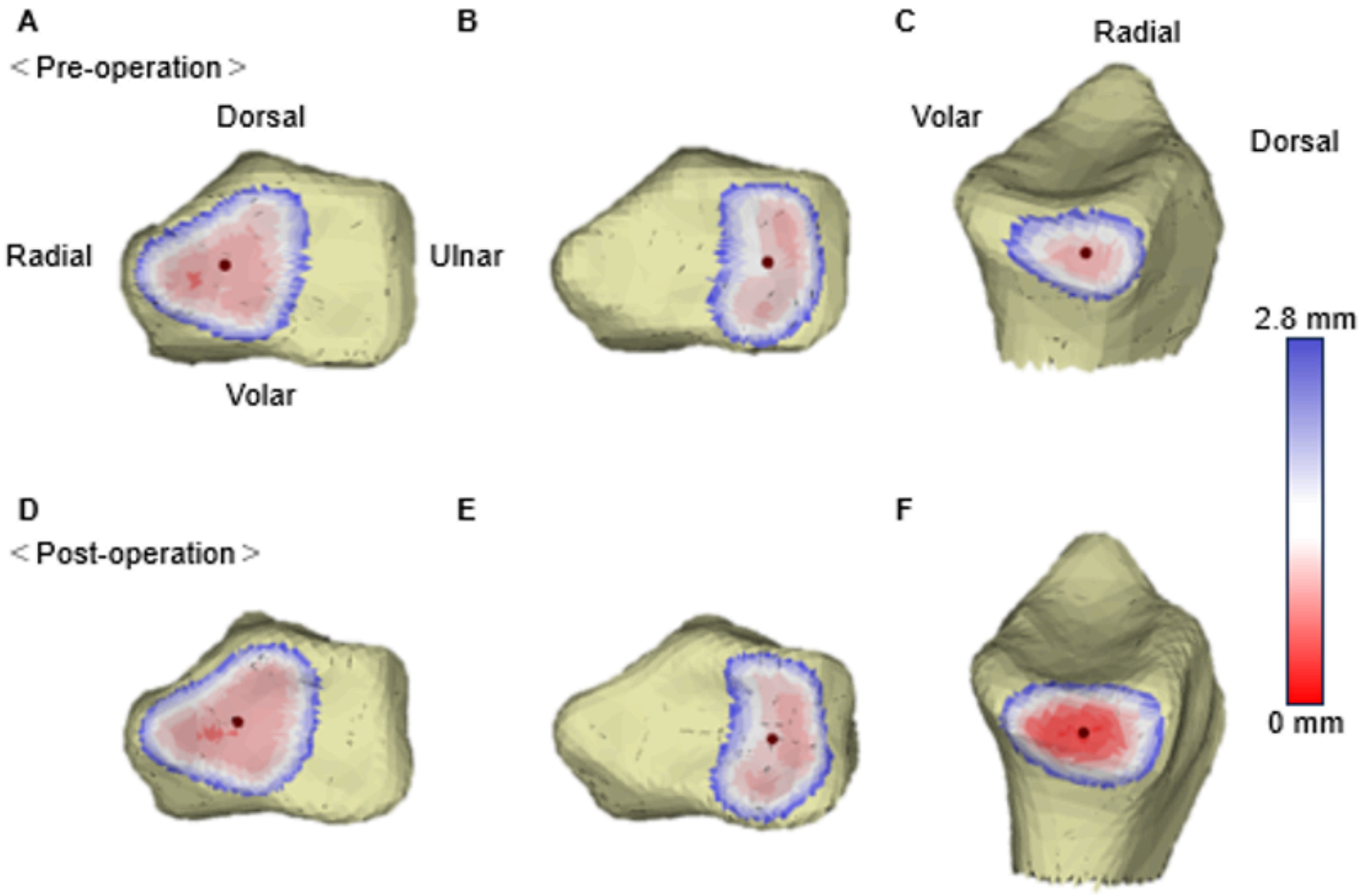


Figure 2

The representative bone models and joint contact area. (A) Preoperative radioscaphoid joint, (B) radiolunate joint, (C) distal radioulnar joint, (D) postoperative radioscaphoid joint, (E) radiolunate joint, (F) distal radioulnar joint contact areas. Wide and narrow joint spaces are shown as blue and red areas, respectively. The black dot indicates the centroid of the joint contact area.

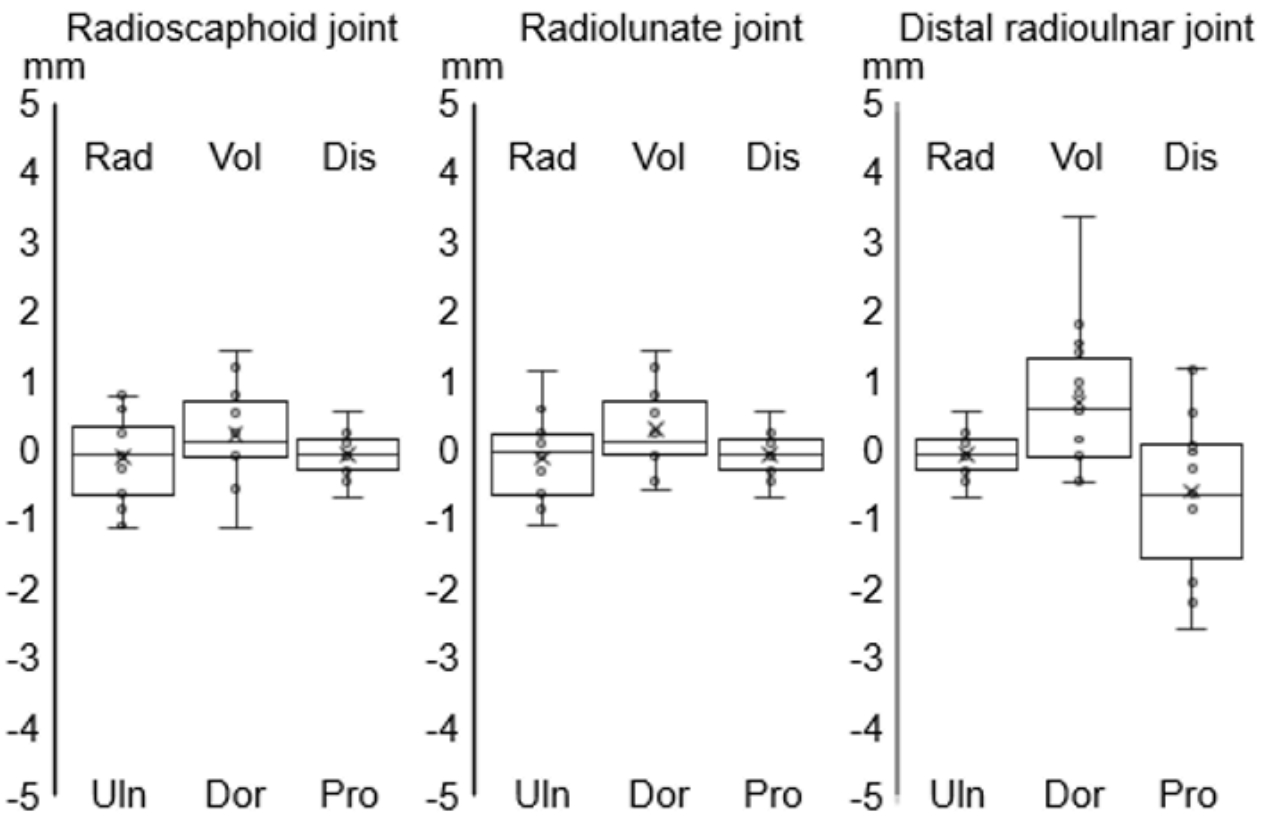


Figure 3

Postoperative translation of the centroid of the joint contact area. Rad: radial, Uln: ulnar, Vol: volar, Dor: dorsal, Dis: distal, Pro: proximal.

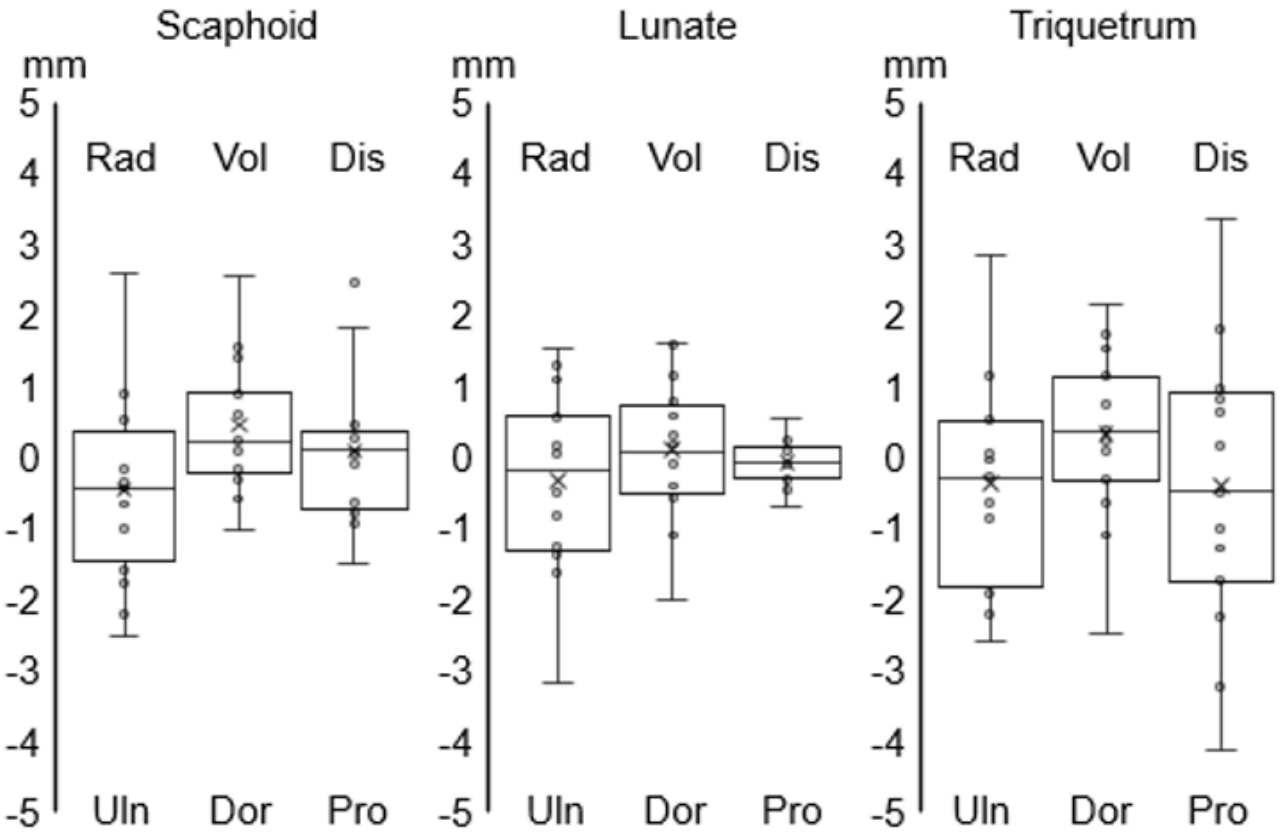


Figure 4

Postoperative translation of the centroid of the carpal bone. Rad: radial, Uln: ulnar, Vol: volar, Dor: dorsal, Dis: distal, Pro: proximal.